Progress In Electromagnetics Research B, Vol. 59, 257–267, 2014

Linear Momentum Density of a General Lorentz-Gauss Vortex Beam in Free Space

Yiqing Xu and Guoquan Zhou*

Abstract—Based on the Collins integral, an analytical expression of a general Lorentz-Gauss vortex beam propagating in free space is derived, which allows one to calculate the linear momentum density of a general Lorentz-Gauss vortex beam in free space. The linear momentum density distribution of a general Lorentz-Gauss vortex beam propagating in free space is graphically demonstrated. The x- and y-components of the linear momentum density are composed of two lobes with the equivalent area and the opposite sign. Therefore, the overall x- and y-components of the linear momentum in an arbitrary reference plane are equal to zero. The longitudinal component of the linear momentum density is proportional to the intensity distribution. The influences of the Gaussian waist, the width parameters of the Lorentzian part, the axial propagation distance, and the topological charge on the linear momentum density distribution of a general Lorentz-Gauss vortex beam in free space are examined in detail.

1. INTRODUCTION

Due to the highly angular spread, Lorentz-Gauss beams have been introduced to describe the radiation emitted by a single mode diode laser [1, 2]. The symmetry properties, the focal shift, the beam propagation factor, and the Wigner distribution function of Lorentz-Gauss beams have been investigated, respectively [3–7]. Propagation of Lorentz-Gauss beams in uniaxial crystals orthogonal to the optical axis, through an apertured fractional Fourier transform optical system, in a turbulent atmosphere, and in Kerr medium has also been examined [8–11]. The virtual source for generation of the rotationally symmetric Lorentz-Gauss beam has been identified [12]. The Lorentz-Gauss beam can be used to trap the particles with a refractive index larger than that of the ambient [13]. Also, Lorentz-Gauss beams have been extended to the partially coherent case [14–16].

If the radiation emitted by a single mode diode laser goes through a spiral phase plate, it becomes a Lorentz-Gauss vortex beam [17]. The wave-front phase of the Lorentz-Gauss vortex beam can be modulated by the spiral phase plate. The advantage of a Lorentz-Gauss vortex beam over the Loretnz-Gauss beam is that it has a twisted phase front and zero intensity in the centre region of the beam profile. The fractional Fourier transform of a Lorentz-Gauss vortex beam has been investigated [18]. Focusing properties of the linearly polarized Lorentz-Gauss beam with one on-axis optical vortex has been studied by means of the vector diffraction theory [19]. Nonparaxial propagation of Lorentz-Gauss vortex beams has been demonstrated in uniaxial crystals orthogonal to the optical axis [20]. The propagation properties of a Lorentz-Gauss vortex beam has been also investigated in a turbulent atmosphere [21]. The linear momentum density is one of the most significant mechanical parameters [22, 23]. A couple of simple quasistatic electromagnetic systems in which the density of electromagnetic linear momentum can be easily computed have been discussed in Ref. [24]. The linear momentum of the electromagnetic field has been examined in magnetic media, and an interesting result of the analysis

Received 21 February 2014, Accepted 27 April 2014, Scheduled 30 April 2014
* Corresponding author: Guoquan Zhou (zhouguoquan178@sohu.com).
The authors are with the School of Sciences, Zhejiang A & F University, Lin'an 311300, China.

is the identification of an "intrinsic" mechanical momentum density analogous to the electromagnetic momentum density [25]. The acquisition of the linear momentum density distribution contributes to the understanding of the vortex dynamics characteristics. As to a practical vortex especially having complex topological structure, it is difficult to accurately measure the spatial distribution of the linear momentum through the experimental method. In the remainder of this paper, therefore, we depict the linear momentum density distribution of a general Lorentz-Gauss vortex beam in free space by means of numerical calculations.

2. LINEAR MOMENTUM DENSITY OF A GENERAL LORENTZ-GAUSS VORTEX BEAM IN FREE SPACE

In the Cartesian coordinate system, the z-axis is taken to be the propagation axis. The general Lorentz-Gauss vortex beam in the source plane $z = 0$ is described by

$$U(x_0, y_0, 0) = \frac{w_{0x} w_{0y} (x_0 + i y_0)^M}{(w_{0x}^2 + x_0^2)(w_{0y}^2 + y_0^2)} \exp\left(-\frac{x_0^2 + y_0^2}{w_0^2}\right), \tag{1}$$

where w_0 is the waist of the Gaussian part. w_{0x} and w_{0y} are the width parameters of the Lorentzian part in the x- and y-directions, respectively. M is the topological charge and is assumed to be a positive integer. The Lorentz distribution can be expanded into the linear superposition of Hermite-Gaussian functions [26]:

$$\frac{1}{(w_{0x}^2 + x_0^2)(w_{0y}^2 + y_0^2)} = \frac{\pi}{2 w_{0x}^2 w_{0y}^2} \sum_{m=0}^{N} \sum_{n=0}^{N} \sigma_{2m} \sigma_{2n} H_{2m}\left(\frac{x_0}{w_{0x}}\right) H_{2n}\left(\frac{y_0}{w_{0y}}\right) \exp\left(-\frac{x_0^2}{2 w_{0x}^2} - \frac{y_0^2}{2 w_{0y}^2}\right), \tag{2}$$

where N is the term number of the expansion. H_{2m} and H_{2n} are the $2m$-th and $2n$-th order Hermite polynomials, respectively. The weight coefficients σ_{2m} and σ_{2n} are given by [26]

$$\begin{aligned} \sigma_{2m} = \frac{(-1)^m \sqrt{2}}{2^{2m}} \Bigg\{ & \frac{1}{m!} \operatorname{erfc}\left(\frac{\sqrt{2}}{2}\right) \exp\left(\frac{1}{2}\right) + \sum_{n_1=1}^{m} \frac{2^{2n_1}}{(2n_1)!(m-n_1)!} \Bigg[\operatorname{erfc}\left(\frac{\sqrt{2}}{2}\right) \exp\left(\frac{1}{2}\right) \\ & + \sqrt{\frac{2}{\pi}} \sum_{n_2=1}^{n_1} (-1)^{n_2} (2n_2 - 3)!! \Bigg] \Bigg\}, \end{aligned} \tag{3}$$

where erfc(.) is the complementary error function. With increasing the even number $2m$, σ_{2m} dramatically decreases, which is shown in Table 1 [26].

Using the following expansion [27]:

$$(x_0 + i y_0)^M = \sum_{l=0}^{M} \frac{M! i^l}{l!(M-l)!} x_0^{M-l} y_0^l, \tag{4}$$

the Lorentz-Gauss vortex beam in the source plane can be rewritten as follows:

$$U(x_0, y_0, 0) = \frac{\pi}{2 w_{0x} w_{0y}} \sum_{l=0}^{M} \sum_{m=0}^{N} \sum_{n=0}^{N} \frac{M! i^l \sigma_{2m} \sigma_{2n}}{l!(M-l)!} x_0^{M-l} y_0^l H_{2m}\left(\frac{x_0}{w_{0x}}\right) H_{2n}\left(\frac{y_0}{w_{0y}}\right) \exp\left(-\frac{x_0^2}{u_x^2} - \frac{y_0^2}{u_y^2}\right), \tag{5}$$

with u_x and u_y being given by

$$\frac{1}{u_j^2} = \frac{1}{w_0^2} + \frac{1}{2 w_{0j}^2}, \tag{6}$$

where $j = x$ or y. The propagation of a Lorentz-Gauss vortex beam in free space is described by the Collins integral formula:

$$U(x, y, z) = \frac{\exp(ikz)}{i\lambda z} \int_{-\infty}^{\infty} \int_{-\infty}^{\infty} U(x_0, y_0, 0) \exp\left\{\frac{ik}{2z}\left[(x_0^2 + y_0^2) - 2(x x_0 + y y_0) + (x^2 + y^2)\right]\right\} dx_0 dy_0, \tag{7}$$

Table 1. Values of the weight coefficient σ_{2m}.

m	σ_{2m}
0	0.7399
1	0.9298×10^{-2}
2	0.5382×10^{-2}
3	0.1112×10^{-3}
4	0.1356×10^{-4}
5	0.3008×10^{-6}
6	0.1769×10^{-7}
7	0.3773×10^{-9}
8	0.1415×10^{-10}
9	0.2782×10^{-12}
10	0.7633×10^{-14}
11	0.1361×10^{-15}
12	0.2958×10^{-17}
13	0.4764×10^{-19}
14	0.8608×10^{-21}
15	0.1255×10^{-22}
16	0.1948×10^{-24}
17	0.2578×10^{-26}
18	0.3522×10^{-28}
19	0.4264×10^{-30}
20	0.5270×10^{-32}

where $k = 2\pi/\lambda$ is the wave number with λ being the optical wavelength. Using the following mathematical formulae [27]:

$$H_{2m}(x)=\sum_{s=0}^{m}\frac{(-1)^s(2m)!}{s!(2m-2s)!}(2x)^{2m-2s}, \tag{8}$$

$$\int_{-\infty}^{\infty}x^n\exp(-bx^2+2cx)dx=n!\sqrt{\frac{\pi}{b}}\left(\frac{c}{b}\right)^n\exp\left(\frac{c^2}{b}\right)\sum_{u=0}^{[n/2]}\frac{1}{u!(n-2u)!}\left(\frac{b}{4c^2}\right)^u, \tag{9}$$

where $[n/2]$ gives the greatest integer less than or equal to $n/2$, one can obtain the analytical expression of a general Lorentz-Gauss vortex beam in free space

$$\begin{aligned}U(x,y,z)=&\frac{\pi k}{4izw_{0x}w_{0y}\sqrt{b_xb_y}}\exp\left[-\frac{k^2x^2}{4b_xz^2}-\frac{k^2y^2}{4b_yz^2}+\frac{ik(x^2+y^2)}{2z}+ikz\right]\sum_{l=0}^{M}\sum_{m=0}^{N}\sum_{n=0}^{N}\sum_{s_1=0}^{m}\sum_{s_2=0}^{n}\frac{(-1)^{s_1+s_2}i^l\sigma_{2m}}{l!(M-l)!s_1!}\\&\times\frac{\sigma_{2n}M!(2m)!(2n)!2^{2m+2n-2s_1-2s_2}(M+2m-l-2s_1)!(l+2n-2s_2)!}{(2m-2s_1)!s_2!(2n-2s_2)!w_{0x}^{2m-2s_1}w_{0y}^{2n-2s_2}}\left(-\frac{ikx}{2b_xz}\right)^{M+2m-l-2s_1}\\&\times\left(-\frac{iky}{2b_yz}\right)^{l+2n-2s_2}\sum_{u_1=0}^{[(M+2m-l-2s_1)/2]}\frac{1}{u_1!(M+2m-l-2s_1-2u_1)!}\left(-\frac{b_xz^2}{k^2x^2}\right)^{u_1}\\&\times\sum_{u_2=0}^{[(l+2n-2s_2)/2]}\frac{1}{u_2!(l+2n-2s_2-2u_2)!}\left(-\frac{b_yz^2}{k^2y^2}\right)^{u_2},\end{aligned} \tag{10}$$

with the auxiliary parameters b_x and b_y being defined as follows:

$$b_j=\frac{1}{w_0^2}+\frac{1}{2w_{0j}^2}-\frac{ik}{2z}. \tag{11}$$

The linear momentum density of a general Lorentz-Gauss vortex beam yields [24]

$$\mathbf{P} = P_x\mathbf{e}_x + P_y\mathbf{e}_y + P_z\mathbf{e}_z, \tag{12}$$

with P_x, P_y, and P_z being given by [28]

$$P_x = \frac{i\varepsilon_0}{\omega}\left[U(x,y,z)\frac{\partial U^*(x,y,z)}{\partial x} - U^*(x,y,z)\frac{\partial U(x,y,z)}{\partial x}\right], \tag{13}$$

$$P_y = \frac{i\varepsilon_0}{\omega}\left[U(x,y,z)\frac{\partial U^*(x,y,z)}{\partial y} - U^*(x,y,z)\frac{\partial U(x,y,z)}{\partial y}\right], \tag{14}$$

$$P_z = \frac{\varepsilon_0 k}{\omega}U(x,y,z)U^*(x,y,z), \tag{15}$$

where $\mathbf{e}_x$, $\mathbf{e}_y$, and $\mathbf{e}_z$ are three unit vectors in the x-, y-, and z-directions, respectively. ω is the circular frequency, and ε_0 is the electric permittivity of vacuum. The asterisk denotes the complex conjugation. Inserting Eq. (10) into Eqs. (13)–(15), one can calculate the linear momentum density distribution of a general Lorentz-Gauss vortex beam in free space.

3. NUMERICAL CALCULATIONS AND ANALYSES

The linear momentum density of a general Lorentz-Gauss vortex beam in free space are determined by the Gaussian waist, the width parameters of the Lorentzian part, the axial propagating distance, and the topological charge. First, we investigate the effects of the Gaussian waist, the width parameters of the Lorentzian part, and the axial propagating distance. The linear momentum density distributions of a general Lorentz-Gauss vortex beam in free space are shown in Figs. 1–6. The optical wavelength is set to be $\lambda = 0.8\,\mu\text{m}$. The topological charge M is fixed and is equal to 3 in Figs. 1–6. $w_0 = 2\,\text{mm}$, $w_{0x} = w_{0y} = 1\,\text{mm}$, and the reference plane is the near field plane $z = z_r$ in Fig. 1. $z_r = kw_0^2/2$ is the confocal parameter of the Gaussian part. The x-component of the linear momentum density is composed of two lobes, which somewhat deviate from the horizontal direction. The areas of the two lobes are equivalent. However, the signs of the linear momentum density in the two lobes are opposite. Therefore, the overall x-component of the linear momentum in the reference plane $z = z_r$ is zero. The y-component of the linear momentum density is also comprised of two lobes, which somewhat deviate from the vertical direction. Also, the overall y-component of the linear momentum in the reference plane $z = z_r$ is zero. The two lobes in the x- and y-components of the linear momentum density are irregular. The y-component of the linear momentum density distribution can be viewed as the x-component of the linear momentum density distribution rotating 90° counterclockwisely. Eq. (15) denotes that the longitudinal component of the linear momentum density is proportional to the intensity distribution. The longitudinal component of the linear momentum density takes on the Lorentzian distribution with a cross-shape dark region, and the bright ring around the dark region is not uniform. Moreover, the Lorentzian distribution tilts to the right. In this case, the effect of the Lorentzian part is predominant. Fig. 1 corresponds to the case of the Gaussian waist being larger than the width parameters of the Lorentzian part. Now, we consider the other case of the Gaussian waist being smaller than the width parameters of the Lorentzian part. In Fig. 2, $w_0 = 1\,\text{mm}$, $w_{0x} = w_{0y} = 2\,\text{mm}$, and other parameters are the same as those in Fig. 1. The two lobes of the x- and y-components of the linear momentum density in Fig. 2 are regular and are similar to the crescent. The two lobes of the x-component of the linear momentum density are oriented in the 135° diagonal direction with respect to the x-axis. The two lobes of the y-component of the linear momentum density are oriented in the 45° diagonal direction with respect to the x-axis. Of course, the overall traversal components of the linear momentum are verified to be zero. The longitudinal component of the linear momentum density takes on the Gaussian distribution with a central dark region. In this case, the influence of the Gaussian part is predominant.

The results of the reference plane $z = 3z_r$ are shown in Fig. 3, where the other paramors are the same as those in Fig. 1. Compared to Fig. 1, the linear momentum density distribution rotates counterclockwisely with increasing the axial propagation distance. The two lobes of the x-component of the linear momentum density are oriented in the horizontal direction. The two lobes of the y-component of the linear momentum density are oriented in the vertical direction. The two lobes become more regular upon propagation. With increasing the axial propagation distance, the magnitude of the linear

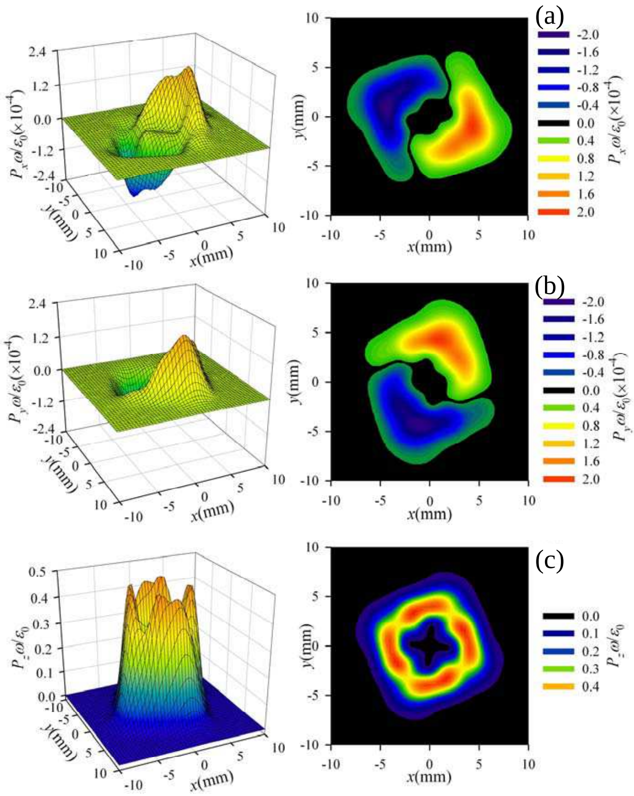

Figure 1. The linear momentum density distributions of a general Lorentz-Gauss vortex beam in the near field $z = z_r$. $w_0 = 2\,\mathrm{mm}$, $w_{0x} = w_{0y} = 1\,\mathrm{mm}$, and $M = 3$.

momentum density decreases. The non-uniformity in the bright ring of the longitudinal component of the linear momentum density has been improved. The results of the reference plane $z = 3z_r$ is shown in Fig. 4, where the other parameters are the same as those in Fig. 2. Compared to Fig. 2, the linear momentum density distribution rotates counterclockwisely for some degree. However, the two lobes of the x-component of the linear momentum density still seriously deviate from the horizontal direction, and the two lobes of the y-component of the linear momentum density seriously deviate from the vertical direction. The reference plane in Fig. 5 is the far field $z = 15z_r$, and the rest of the parameters are the same as those in Fig. 1. The two lobes of the x-component of the linear momentum density are oriented in the horizontal direction. The two lobes of the y-component of the linear momentum density are oriented in the vertical direction. The lobes are very regular. The tilt of longitudinal component of the linear momentum density disappears. The reference plane in Fig. 6 is also the far field $z = 15z_r$, and the rest of the parameters are the same as those in Fig. 2. The two lobes of the x- and y-components of the linear momentum density are oriented in the horizontal and the vertical directions, respectively.

Finally, we investigate the influence of the topological charge on the linear momentum density distribution of Lorentz-Gauss vortex beams propagating in free space. $M = 4$ in Fig. 7, and the rest of the parameters are the same as those in Fig. 1. In the near field, however, a faint lobe appears in the central region of the longitudinal component of the linear momentum density. With increasing the topological charge, the non-uniformity in the bright ring around the dark region of the longitudinal component of the linear momentum density increases. The reference plane in Figs. 8 and 9 is $z = 3z_r$ and $z = 15z_r$, respectively. Other parameters besides the axial propagation distance are the same as those in Fig. 7. With increasing the axial propagation distance, the magnitude of the lobe in the central region of the longitudinal component of the linear momentum density is enhanced, and the non-uniformity in the bright ring of the longitudinal component of the linear momentum density is also improved. When the Gaussian waist is smaller than the width parameters of the Lorentzian part, the faint lobe will not appear in the central region of the longitudinal component of the linear momentum density, and the corresponding figure is omitted to save space.

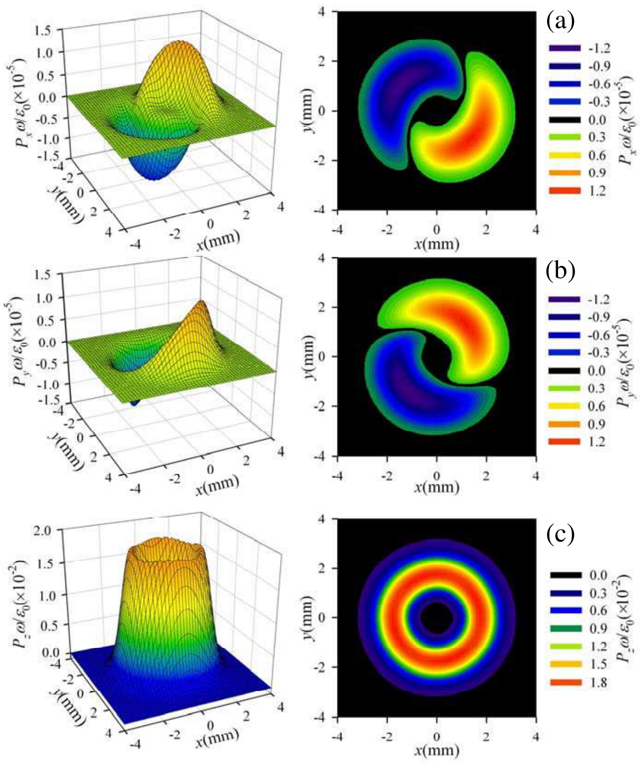

Figure 2. The momentum density distributions of a general Lorentz-Gauss vortex beam in the near field $z = z_r$. $w_0 = 1\,\mathrm{mm}$, $w_{0x} = w_{0y} = 2\,\mathrm{mm}$, and $M = 3$.

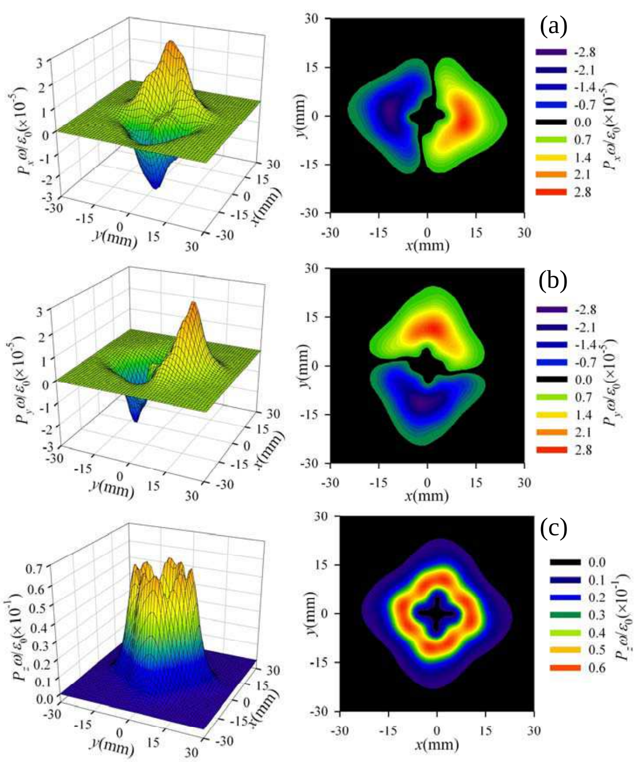

Figure 3. The momentum density distributions of a general Lorentz-Gauss vortex beam in the reference plane $z = 3z_r$. $w_0 = 2\,\mathrm{mm}$, $w_{0x} = w_{0y} = 1\,\mathrm{mm}$, and $M = 3$.

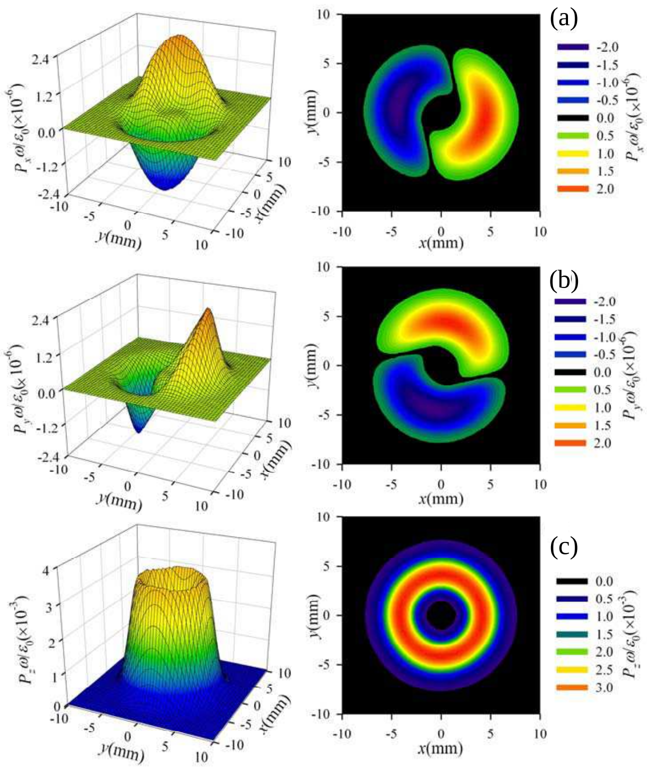

Figure 4. The momentum density distributions of a general Lorentz-Gauss vortex beam in the reference plane $z = 3z_r$. $w_0 = 1\,\mathrm{mm}$, $w_{0x} = w_{0y} = 2\,\mathrm{mm}$, and $M = 3$.

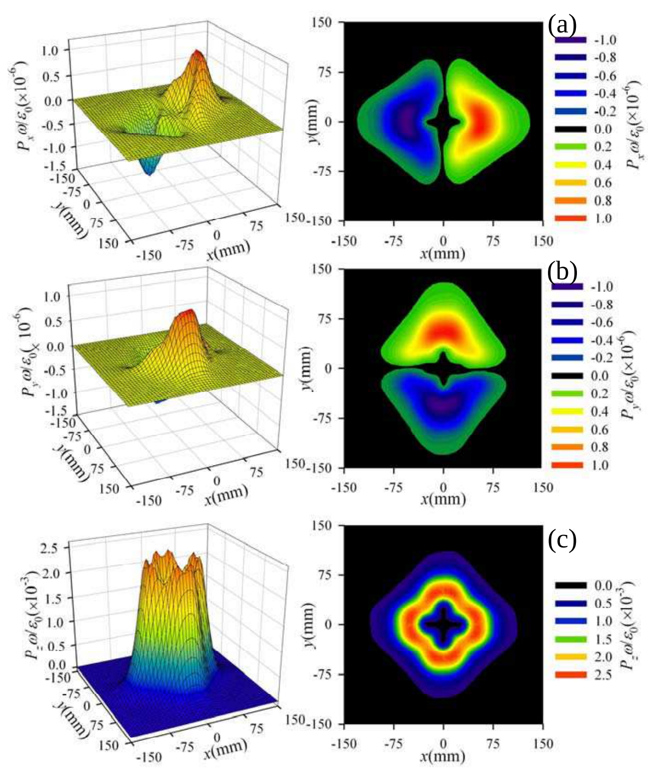

Figure 5. The momentum density distributions of a general Lorentz-Gauss vortex beam in the far field $z = 15z_r$. $w_0 = 2\,\mathrm{mm}$, $w_{0x} = w_{0y} = 1\,\mathrm{mm}$, and $M = 3$.

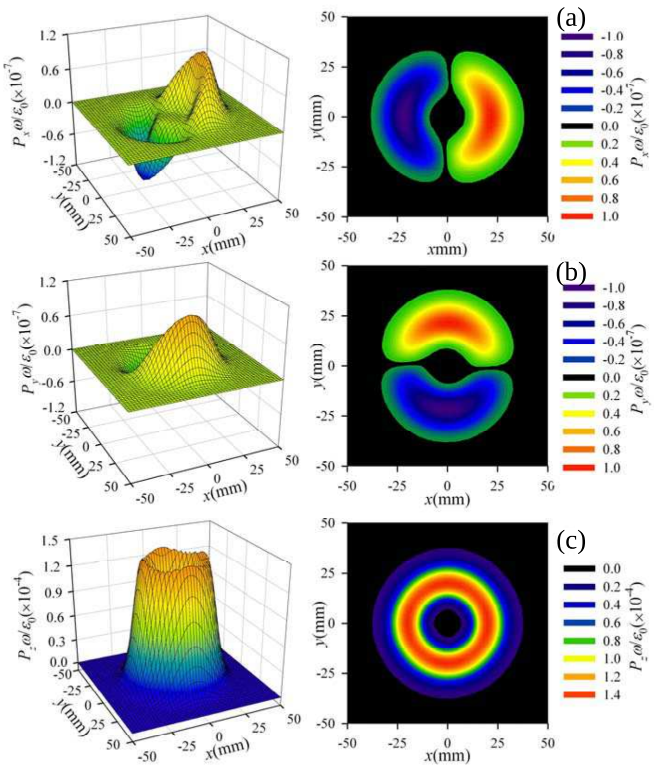

Figure 6. The momentum density distributions of a general Lorentz-Gauss vortex beam in the far field $z = 15z_r$. $w_0 = 1\,\mathrm{mm}$, $w_{0x} = w_{0y} = 2\,\mathrm{mm}$, and $M = 3$.

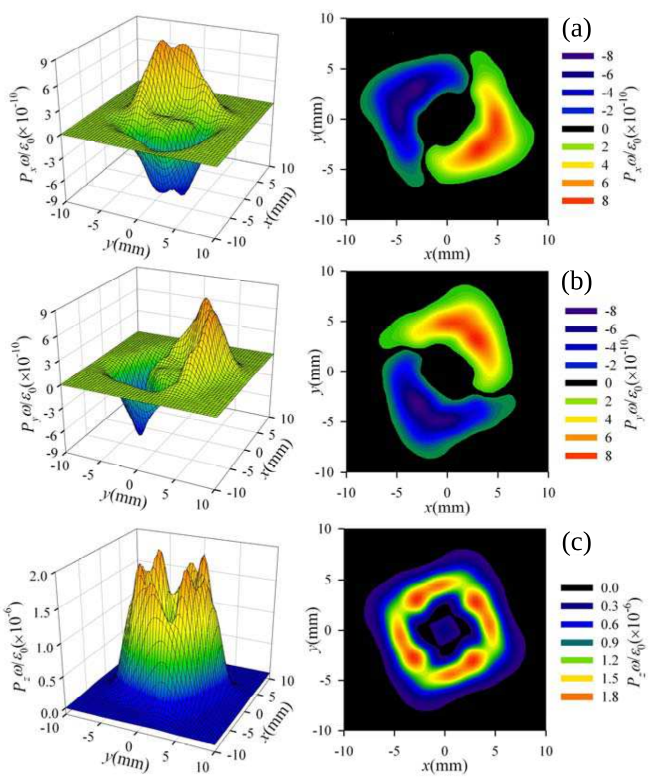

Figure 7. The momentum density distributions of a general Lorentz-Gauss vortex beam in the near field $z = z_r$. $w_0 = 2\,\mathrm{mm}$, $w_{0x} = w_{0y} = 1\,\mathrm{mm}$, and $M = 4$.

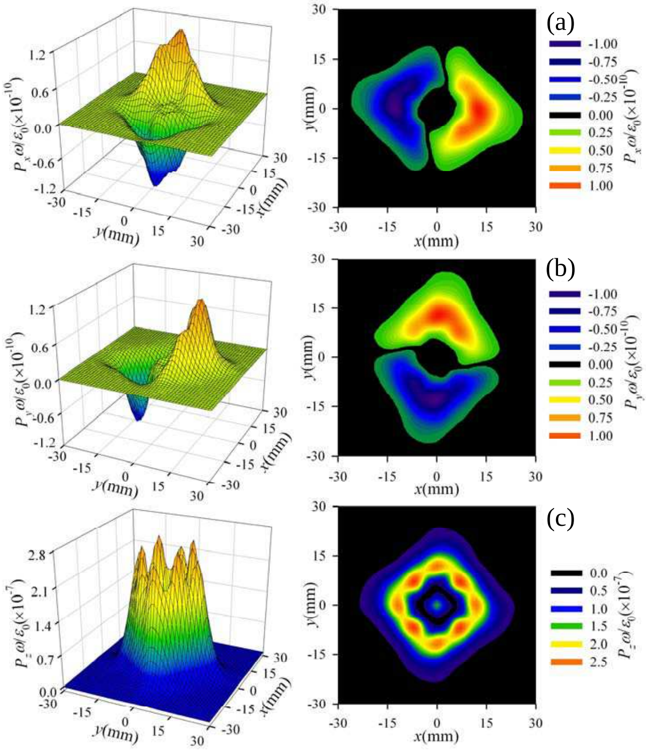

Figure 8. The momentum density distributions of a general Lorentz-Gauss vortex beam in the reference plane $z = 3z_r$. $w_0 = 2\,\text{mm}$, $w_{0x} = w_{0y} = 1\,\text{mm}$, and $M = 3$.

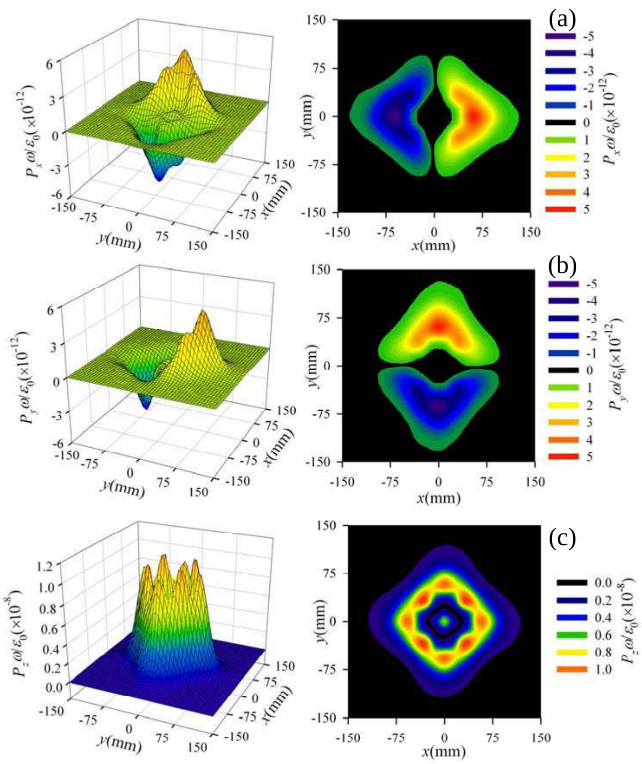

Figure 9. The momentum density distributions of a general Lorentz-Gauss vortex beam in the far field $z = 15z_r$. $w_0 = 2\,\text{mm}$, $w_{0x} = w_{0y} = 1\,\text{mm}$, and $M = 4$.

4. CONCLUSIONS

The analytical expression of general Lorentz-Gauss vortex beams propagating in free space is derived, which allows one to calculate the linear momentum density of a general Lorentz-Gauss vortex beam in free space. The influences of the Gaussian waist, width parameters of the Lorentzian part, axial propagation distance, and topological charge on the linear momentum density distribution of Lorentz-Gauss vortex beams propagating in free space are examined, respectively. The x- and y-components of the linear momentum density is composed of two lobes with the equivalent areas. However, the signs of the linear momentum density in the two lobes are opposite. Therefore, the overall x- and y-components of the linear momentum in an arbitrary reference plane are equal to zero. When the width parameters of the Lorentzian part are smaller than the Gaussian waist, the two lobes in the x- and y-components of the linear momentum density are irregular, and the longitudinal component of the linear momentum density takes on the Lorentzian distribution with a cross-shape dark region. Moreover, the Lorentzian distribution tilts to the right, and the bright ring around the cross-shape dark region is not uniform. When the Gaussian waist is smaller than the width parameters of the Lorentzian part, the two lobes of the x- and y-components of the linear momentum density are regular and are similar to the crescent. In this case, the longitudinal component of the linear momentum density takes on the Gaussian distribution with a central dark region. With increasing the axial propagation distance, the magnitude of the linear momentum density decreases, and the linear momentum density distribution rotates counterclockwisely. In the far field, the two lobes of the x-component of the linear momentum density are oriented in the horizontal direction, and the two lobes of the y-component of the linear momentum density are oriented in the vertical direction. The tilt in the longitudinal component of the linear momentum density disappears. In the case of the width parameters of the Lorentzian part being smaller than the Gaussian waist and topological charge being larger than 3, a faint lobe appears in the central region of the longitudinal component of the linear momentum density, and the magnitude of the faint lobe increases upon propagation. With increasing the topological charge, moreover, the non-uniformity in the bright ring of the longitudinal component of the linear momentum density is also improved. The present research is useful to the decoding of the information in optical communications. Also, it is beneficial to optical trapping, guiding, and manipulation of microscopic particles involving the single mode diode laser beams.

ACKNOWLEDGMENT

This research was supported by the National Natural Science Foundation of China under Grant No. 10974179 and Zhejiang Provincial Natural Science Foundation of China under Grant No. Y1090073.

REFERENCES

1. Naqwi, A. and F. Durst, "Focus of diode laser beams: A simple mathematical model," *Appl. Opt.*, Vol. 29, 1780–1785, 1990.
2. Yang, J., T. Chen, G. Ding, and X. Yuan, "Focusing of diode laser beams: A partially coherent Lorentz model," *Proc. SPIE*, Vol. 6824, 68240A, 2008.
3. Gawhary, O. E. and S. Severini, "Lorentz beams and symmetry properties in paraxial optics," *J. Opt. A: Pure Appl. Opt.*, Vol. 8, 409–414, 2006.
4. Zhou, G., "Focal shift of focused truncated Lorentz-Gauss beam," *J. Opt. Soc. Am. A*, Vol. 25, 2594–2599, 2008.
5. Zhou, G., "Beam propagation factors of a Lorentz-Gauss beam," *Appl. Phys. B*, Vol. 96, 149–153, 2009.
6. Zhou, G. and R. Chen, "Wigner distribution function of Lorentz and Lorentz-Gauss beams through a paraxial ABCD optical system," *Appl. Phys. B*, Vol. 107, 183–193, 2012.
7. Torre, A., "Wigner distribution function of Lorentz-Gauss beams: A note," *Appl. Phys. B*, Vol. 109, 671–681 2012.

8. Zhao, C. and Y. Cai, "Paraxial propagation of Lorentz and Lorentz-Gauss beams in uniaxial crystals orthogonal to the optical axis," *J. Mod. Opt.*, Vol. 57, 375–384, 2010.
9. Du, W., C. Zhao, and Y. Cai, "Propagation of Lorentz and Lorentz-Gauss beams through an apertured fractional Fourier transform optical system," *Opt. Lasers in Eng.*, Vol. 49, 25–31, 2011.
10. Zhou., G., and X. Chu, "Average intensity and spreading of a Lorentz-Gauss beam in turbulent atmosphere," *Opt. Express*, Vol.18, 726–731, 2010.
11. Chen, R. and C. H. R. Ooi, "Evolution and collapse of a Lorentz beam in Kerr medium," *Progress In Electromagnetics Research*, Vol. 121, 39–52, 2011.
12. Sun, Q., A. Li, K. Zhou, Z. Liu, G. Fang, and S. Liu, "Virtual source for rotational symmetric Lorentz-Gaussian beam," *Chin. Opt. Lett.*, Vol. 10, 062601, 2012.
13. Jiang, Y., K. Huang, and X. Lu, "Radiation force of highly focused Lorentz-Gauss beams on a Rayleigh particle," *Opt. Express*, Vol. 19, 9708–9713, 2011.
14. Zhou, G., "Propagation of a partially coherent Lorentz-Gauss beam through a paraxial ABCD optical system," *Opt. Express*, Vol. 18, 4637–4643, 2010.
15. Eyyuboğlu, H. T., "Partially coherent Lorentz-Gaussian beam and its scintillations," *Appl. Phys. B*, Vol. 103, 755–762, 2011.
16. Zhao, C. and Y. Cai, "Propagation of partially coherent Lorentz and Lorentz-Gauss beams through a paraxial ABCD optical system in a turbulent atmosphere," *J. Mod. Opt.*, Vol. 58, 810–818, 2011.
17. Ni, Y. and G. Zhou, "Propagation of a Lorentz-Gauss vortex beam through a paraxial ABCD optical system," *Opt. Commun.*, Vol. 291, 19–25, 2013.
18. Zhou, G., X. Wang, and X. Chu, "Fractional Fourier transform of Lorentz-Gauss vortex beams," *Science China-Physics, Mechanics & Astronomy*, Vol. 56, 1487–1494, 2013.
19. Rui, F., D. Zhang, M. Ting, X. Gao, and S. Zhuang, "Focusing of linearly polarized Lorentz-Gauss beam with one optical vortex," *Optik*, Vol. 124, 2969–2973, 2013.
20. Ni, Y. and G. Zhou, "Nonparaxial propagation of Lorentz-Gauss vortex beams in uniaxial crystals orthogonal to the optical axis," *Appl. Phys. B*, Vol. 108, 883–890, 2012.
21. Zhou, G. and G. Ru, "Propagation of a Lorentz-Gauss vortex beam in a turbulent atmosphere," *Progress In Electromagnetics Research*, Vol. 143, 143–163, 2013.
22. Charrier, D. S. H., "Loss of linear momentum in an electrodynamics system: From an analytical approach to simulations," *Progress In Electromagnetics Research M*, Vol. 13, 69–82, 2010.
23. He, Y., J. Shen, and S. He, "Consistent formalism for the momentum of electromagnetic waves in lossless dispersive metamaterials and the conservation of momentum," *Progress In Electromagnetics Research*, Vol. 116, 81–106, 2011.
24. Aguirregabiria, J. M., A. Hernández, and M. Rivas, "Linear momentum density in quasistatic electromagnetic systems," *Eur. J. Phys.*, Vol. 25, 555–567, 2004.
25. Mansuripur, M., "Radiation pressure and the linear momentum of the electromagnetic field in magnetic media," *Opt. Express*, Vol. 15, 13502–13517, 2007.
26. Schmidt, P. P., "A method for the convolution of lineshapes which involve the Lorentz distribution," *J. Phys. B: Atom. Molec. Phys.*, Vol. 9, 2331–2339, 1976.
27. Gradshteyn, I. S. and I. M. Ryzhik, *Table of Integrals, Series, and Products*, Academic Press, New York, 1980.
28. Allen, L., M. W. Beijersbergen, R. J. C. Spreeuw, and J. P. Woerdman, "Orbital angular momentum of light and the transformation of Laguerre-Gaussian laser modes," *Phys. Rev. A*, Vol. 45, 8185–8189, 1992.